



Monoclinic M C vs orthorhombic in [001] and [110] electric-field-cooled Pb (Mg 1 3 Nb 2 3 O 3) – 35 % PbTiO 3 Crystals

Hu Cao, Jiefang Li, D. Viehland, Guangyong Xu, and Gen Shirane

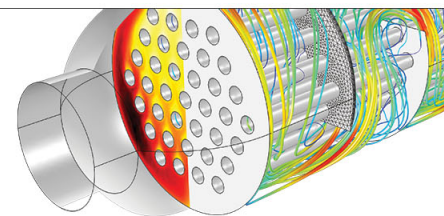
Citation: [Applied Physics Letters](#) **88**, 072915 (2006); doi: 10.1063/1.2175497

View online: <http://dx.doi.org/10.1063/1.2175497>

View Table of Contents: <http://scitation.aip.org/content/aip/journal/apl/88/7?ver=pdfcov>

Published by the [AIP Publishing](#)

Over **700** papers &
presentations on
multiphysics simulation



VIEW NOW ►

 COMSOL

Monoclinic M_C vs orthorhombic in [001] and [110] electric-field-cooled $Pb(Mg_{1/3}Nb_{2/3}O_3)-35\%PbTiO_3$ Crystals

Hu Cao,^{a)} Jiefang Li, and D. Viehland

Department of Materials Science and Engineering, Virginia Tech, Blacksburg, Virginia 24061

Guangyong Xu and Gen Shirane

Physics Department, Brookhaven National Laboratory, Upton, New York 11973

(Received 9 August 2005; accepted 4 January 2006; published online 16 February 2006)

Structural phase transformations in $Pb(Mg_{1/3}Nb_{2/3}O_3)-35\%PbTiO_3$ crystals with an electric field (E) applied along [110] and [001] directions have been performed by x-ray diffraction. In the field-cooling process, a phase transformation sequence of Cubic(C) \rightarrow Tetragonal(T) \rightarrow Orthorhombic(O) was found for E//[110]; whereas a sequence of C \rightarrow T \rightarrow monoclinic(M_C) was found for E//[001]. Our results establish that the stability of M_C relative to O (or limiting M_C) is altered by the direction along which E is applied. © 2006 American Institute of Physics. [DOI: 10.1063/1.2175497]

Relaxor ferroelectric based morphotropic phase boundary crystals, such as $(1-x)Pb(Mg_{1/3}Nb_{2/3}O_3)-xPbTiO_3$ (PMN- $x\%$ PT) and $(1-x)Pb(Zn_{1/3}Nb_{2/3}O_3)-xPbTiO_3$ (PZN- $x\%$ PT), have attracted much interest as high performance piezoelectric actuator and transducer materials.¹ An important breakthrough in understanding the structural origin of these high electromechanical properties was the discovery of ferroelectric monoclinic (M) phases bridging the R and T ones, as first reported for $Pb(Zr_xTi_{1-x})O_3$.²⁻⁴ The monoclinic M_A phase (Cm) has a unique b_m axis along the [110] direction, and a unit cell that is doubled with respect to the primitive cubic one which is rotated 45° about the c axis; whereas, the monoclinic M_C (Pm) has a unique b_m axis along the [010] direction. Both neutron and x-ray powder diffraction measurements have revealed the existence of a M_C phase ($c_M \neq a_M$) in zero-field-cooled (ZFC) PMN- $x\%$ PT⁵⁻⁷ for $31\% \leq x \leq 37\%$. In addition, a monoclinic M_C phase has been observed for (001) field cooled (FC) in PMN-30%PT,⁸ whereas the ZFC state was R.

An orthorhombic (O) phase ($Bmm2$) has also been reported to be induced by a field applied along [001] in PZN- $x\%$ PT for $8 \leq x \leq 10$.^{9,10} This O phase is the limiting case of the monoclinic M_C structure: in the limit of $a_M = c_M$ and $\beta > 90^\circ$, the crystal symmetry becomes O, and the polarization is then fixed to the [110] direction. This O structure has a doubled unit cell, consisting of two M_C primitive cells, with lattice parameters of $a_O = 2a_M \sin(\beta/2)$, $c_O = 2a_M \cos(\beta/2)$, and $b_O = b_M$.^{6,11} Dielectric property studies of PMN-33%PT crystals with E//[110] have reported an intermittently present metastable orthorhombic phase over a narrow temperature range. Polarized light microscopy indicated that this evasive phase was a single domain orthorhombic one.¹² In addition, the P-E and ϵ -E behaviors of ZFC PMN-30%PT¹³ crystals with E along [110] have been reported, upon which was conjectured a field-induced O phase at room temperature. However, structural studies have not yet established the presence of a ferroelectric O phase in PMN- $x\%$ PT, either for E//[001] or E//[110].

In this investigation, we have studied the phase stability of PMN-35%PT crystals for both E//[001] and E//[110] by high-resolution x-ray diffraction (XRD). Our results establish a M_C phase on [001] field cooling, but an O phase (or limiting M_C) on [110] field cooling.

Single crystals of PMN-35%PT with dimension of $3 \times 3 \times 3$ mm³ were obtained from HC Materials (Urbana, IL), and were grown by a top-seeded modified Bridgman method. The PMN-35%PT cube, carefully chosen with $T_c \sim 435$ K, was cut along the pseudocubic (110)/(1 $\bar{1}$ 0)/(001) planes, and was polished to 0.25 μ m. All measurements were performed on the same specimen and consisted of two steps. The first was to apply an electric field along the [001] direction and the second was to apply an electric field along [110]. Gold electrodes were successively deposited on one pair of opposite (001) and (110) faces of the cube. The XRD studies were performed using a Philips MPD high-resolution system equipped with a two bounce hybrid monochromator, an open three-circle Eulerian cradle, and a doomed hot stage. A Ge (220)-cut crystal was used as an analyzer, which had an angular resolution of 0.0068°. The x-ray wavelength was that of Cu K α = 1.5406 Å, and the x-ray generator operated at 45 kV and 40 mA. The penetration depth in the samples was on the order of 10 μ m. In our diffraction studies, we have performed mesh scans around the (002) Bragg reflection in the (HHL) zone, defined by the [110] and [001] vectors; the (220) and (2-20) reflections in the scattering zone defined by the [110] and [1-10] vectors; and (200) in the (HOL) zone, defined by the [100] and [001] vectors. Each measurement cycle was begun by heating up to 550 K to depole the crystal, and measurements subsequently taken on cooling. In this study, we choose the reciprocal lattice unit (or 1 rlu) $a^* = 1.560$ Å⁻¹ ($a = 2\pi/a^* = 4.027$ Å). All mesh scans of (001) and (110) PMN-35%PT shown in this study were plotted in reference to this reciprocal unit.

Figure 1 shows mesh scans taken around the (002) and (200) reflections for [001] FC PMN-35%PT at various temperatures for E=2 kV/cm. At 475 K (data not shown), the (002) and (200) mesh scans did not exhibit splitting, and it was found that $c = a$. Thus, it is clear that the lattice has cubic symmetry. As the temperature was decreased, the (002) and

^{a)} Author to whom correspondence should be addressed; electronic mail: hcao@vt.edu

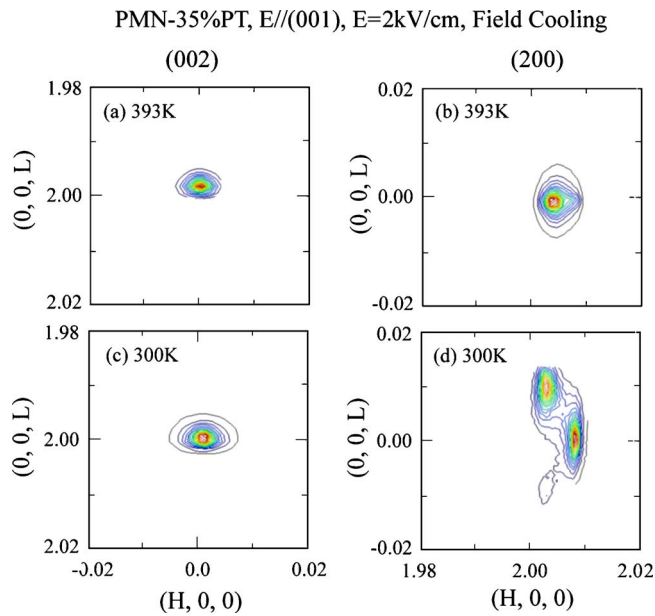


FIG. 1. (Color online) Mesh scans taken around (002) and (200) reflections of PMN-35%PT with $E=2$ kV/cm applied along [001] at 393 and 300 K in the FC condition.

(200) mesh scans both exhibited one peak; but an elongation of the lattice constant c_T and a contraction of a_T were clearly observed, as shown in Fig. 1(a) and 1(b) at $T=393$ K. This indicates that the crystal transforms into a T structure. Upon further decreasing temperature, a second transition to a M_C phase was found, as shown in Figs. 1(c) and 1(d) at 300 K. The (200) peak split into three reflections, (200) twin peaks and one (020) single peak; whereas, the (002) remained as a single reflection.

We also studied the temperature dependence of the lattice parameters for a PMN-35%PT crystal in the [110] field-cooled condition. Relative to [001] FC PMN-35%PT, [110] field cooling results in a more complicated domain configuration. This is because [001] field cooling fixes the prototype c axis, whereas [110] field cooling only fixes the crystallographic [110] direction. To obtain a more comprehensive understanding, we then measured field cooling mesh scans about the (002), (200), (220) and ($\bar{2}\bar{2}0$) reflections for a $E//[110]$ of 2 kV/cm. Figures 2(a)–2(d) show mesh scans at 400 K taken around these four directions, respectively. The (002) reflection [see Fig. 2(a)] only has a single sharp peak. The lattice constant extracted from it was 4.0119 Å. However, the (200) reflection [see Fig. 2(b)] was split into two peaks along the longitudinal direction, with the lattice parameters of $a=4.0122$ Å and $c=4.0361$ Å. The [110] field cooling constrains the polarization in the T phase to the (001) plane. The a_T lattice parameter is then derived from the (002), whereas c_T is obtained from the (200) reflection. Since [110] field cooling fixes the [110] crystallographic orientations, the ($\bar{2}\bar{2}0$) mesh scan [see Fig. 2(c)] splits into two peaks along the transverse direction, but remains as a single peak for the (220) scan [see Fig. 2(d)]. Accordingly, for ($\bar{2}\bar{2}0$) mesh scan, a and b twinning in the (001) plane is only seen along the transverse (220) direction. Our results in Fig. 2 evidence a tetragonal lattice, with 90° domain formation only in the (001) plane, whose polarization is constrained along the [100] and [010] direction.

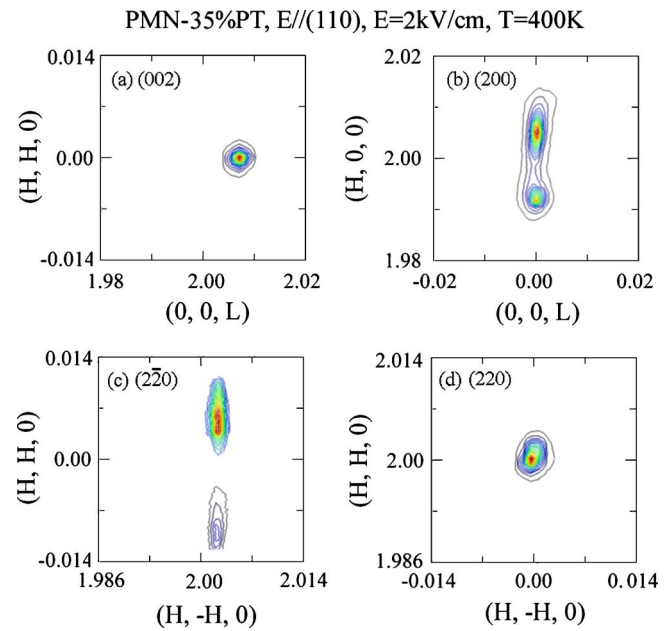


FIG. 2. (Color online) Mesh scans taken around (002), (200), ($\bar{2}\bar{2}0$), and (220) reflections of PMN-35%PT with $E=2$ kV/cm applied along [110] at 400 K in the FC condition.

As the temperature was further decreased on [110] field cooling, the longitudinal splitting in the (200) mesh scan disappeared near 308 K, indicating another phase transformation. Figures 3(a)–3(d) show mesh scans at 303 K within this phase field that were taken about the (002), (200), ($\bar{2}\bar{2}0$), and (220) reflections, respectively. Only a single domain was observed in each of these scans, indicating the presence of a well-developed single domain state throughout the entire crystal. The structure of this phase was determined to be orthorhombic, where the polarization is fixed to the [110]. The lattice parameters of this orthorhombic phase were determined from these mesh scans to be $a_O=5.7055$ Å,

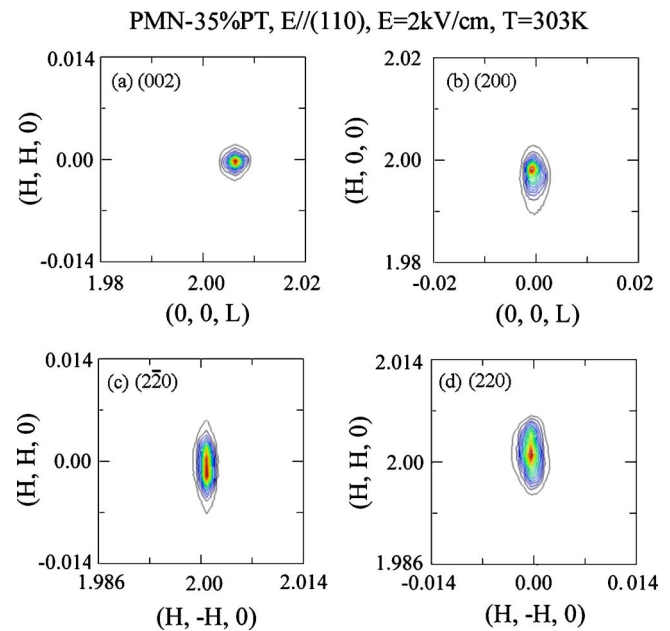


FIG. 3. (Color online) Mesh scans taken around (002), (200), ($\bar{2}\bar{2}0$), and (220) reflections of PMN-35%PT with $E=2$ kV/cm applied along [110] at 303 K in the FC condition.

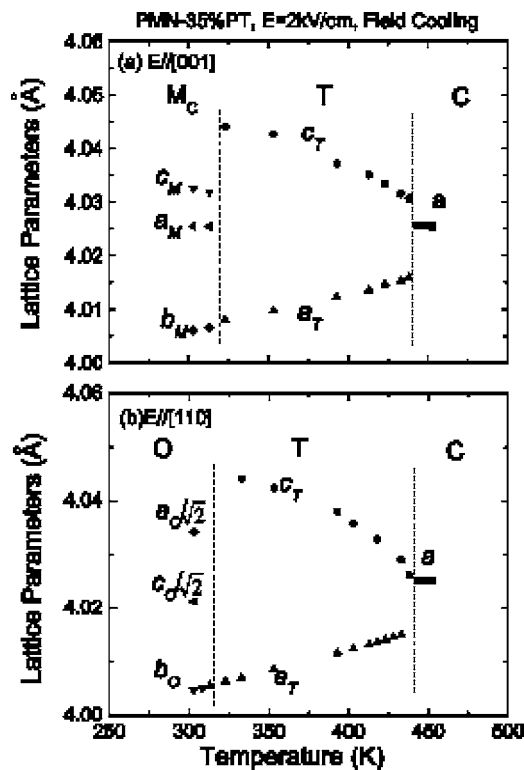


FIG. 4. Temperature dependence of lattice parameters for PMN-35%PT with (a) $E//[001]$ of 2 kV/cm and (b) $E//[110]$ of 2 kV/cm.

$c_O = 5.6870 \text{ \AA}$, and $b_O = 4.0050 \text{ \AA}$, where a_O was extracted from the (220) reflection, c_O from the (2 $\bar{2}$ 0), and b_O from the (002). This O structure has an equivalent limiting M_C primitive cell with the corresponding lattice parameters of $a_M = c_M = 4.0279 \text{ \AA}$, $b_M = 4.005 \text{ \AA}$, and $\beta = 90.186^\circ$.

Figure 4 shows the temperature dependence of the lattice constants for (a) an $E//[001]$ of 2 kV/cm and (b) an $E//[110]$ of 2 kV/cm. The results for the two orientations are identical except in the low temperature region, where [001] field cooling results in M_C , whereas [110] field cooling results in O. The lattice constant c_T (a_T) gradually increased (decreased) as the temperature decreased and suddenly dropped near 308 K. At lower temperatures, [001] field cooling resulted in a $T \rightarrow M_C$ transformation, whereas [110] field

cooling results in a $T \rightarrow O$. It is worth noting that the values of b_M and b_O were both continuous with a_T at their respective $T \rightarrow M_C$ and $T \rightarrow O$ transformations, whereas the values of a_M ($a_O/\sqrt{2}$) and c_M ($c_O/\sqrt{2}$) exhibit sharp decreases at the $T \rightarrow M_C$ ($T \rightarrow O$) transformation relative to c_T . In addition, we found the O phase to be stable on removal of $E//[110]$, and correspondingly the M_C to be stable on removal of $E//[001]$. This illustrates a subtle yet important difference between the ground state of these two field-cooled conditions.

In summary, the sequence of [001] and [110] electric field cooled PMN-35%PT crystals was $C \rightarrow T \rightarrow M_C$ for $E//[001]$, but $C \rightarrow T \rightarrow O$ for $E//[110]$, respectively. Our results establish that the stability of M_C relative to O (or limiting M_C) is altered by the direction along which E is applied.

The authors would like to gratefully acknowledge financial support from the Office of Naval Research under Grant Nos. N000140210340, N000140210126, and MURI N0000140110761. They would like to thank HC Materials for providing the single crystals used in this study.

¹S.-E. Park and T. R. Shroud, J. Appl. Phys. **82**, 1804 (1997).

²B. Noheda, D. E. Cox, G. Shirane, J. A. Gonzalo, L. E. Cross, and S.-E. Park, Appl. Phys. Lett. **74**, 2059 (1999).

³B. Noheda, J. A. Gonzalo, L. E. Cross, R. Guo, S.-E. Park, D. E. Cox, and G. Shirane, Phys. Rev. B **61**, 8687 (2000).

⁴B. Noheda, D. E. Cox, G. Shirane, R. Guo, B. Jones, and L. E. Cross, Phys. Rev. B **63**, 014103 (2000).

⁵B. Noheda, D. E. Cox, G. Shirane, J. Gao, and Z. G. Ye, Phys. Rev. B **66**, 054104 (2002).

⁶J. Kiat, Y. Uesu, B. Dkhil, M. Matsuda, C. Malibert, and G. Calvarin, Phys. Rev. B **65**, 064106 (2002).

⁷A. K. Singh and D. Pandey, J. Phys.: Condens. Matter **13**, L931 (2001).

⁸F. Bai, N. Wang, J. Li, D. Viehland, P. Gehring, G. Xu, and G. Shirane, J. Appl. Phys. **96**, 1620 (2004).

⁹B. Noheda, D. E. Cox, G. Shirane, S. E. Park, L. E. Cross, and Z. Zhong, Phys. Rev. Lett. **86**, 3891 (2001).

¹⁰D. La-Orauttapong, B. Noheda, Z. G. Ye, P. M. Gehring, J. Toulouse, D. E. Cox, and G. Shirane, Phys. Rev. B **65**, 144101 (2002).

¹¹F. Jona and G. Shirane, *Ferroelectric Crystals* (Pergamon, New York, 1962).

¹²Y. Lu, D.-Y. Jeong, Z.-Y. Cheng, Q. M. Zhang, H. Luo, Z. Yin, and D. Viehland, Appl. Phys. Lett. **78**, 3109 (2001).

¹³D. Viehland and J. F. Li, J. Appl. Phys. **92**, 7690 (2002).